



CrossMark  
 click for updates

Cite this: *RSC Adv.*, 2015, 5, 43141

# Highly dispersed molybdenum carbide nanoparticles supported on activated carbon as an efficient catalyst for the hydrodeoxygenation of vanillin

Lili He, Yu Qin, Hui Lou and Ping Chen\*

Characterized by XRD and TEM, highly dispersed molybdenum carbide ( $\text{Mo}_2\text{C}$ ) nanoparticles with a diameter of 1–4 nm were effectively synthesized on activated carbon at 700 °C. The  $\text{Mo}_2\text{C}$ -based catalyst exhibited high activity and stability for the hydrodeoxygenation (HDO) of vanillin under mild conditions (100 °C, 1.0 MPa of  $\text{H}_2$ , 3 h) in aqueous solution. According to the distribution of products with time, a HDO mechanism involving vanillyl alcohol as an intermediate product was proposed. Moreover, after being recycled several times, the loss of catalytic activity was negligible, which demonstrated that the  $\text{Mo}_2\text{C}$ -based catalyst had the property of resistance to deactivation.

Received 15th January 2015  
 Accepted 15th April 2015

DOI: 10.1039/c5ra00866b

[www.rsc.org/advances](http://www.rsc.org/advances)

## 1. Introduction

Nowadays, the continuous requirement for energy, which is mainly obtained from fossil fuel sources, has caused the exhausting of petroleum reserves. With the arising world-wide environmental concerns, the search for renewable feedstocks as a replacement for traditional fossil fuels to meet the huge future needs is required urgently. Due to their environmental-friendliness, world-wide abundance and renewable nature within a relatively short cycle,<sup>1,2</sup> bio-oils, as a prospective resource for replacing fossil fuels have attracted more and more attention. However, due to their high oxygen content,<sup>3</sup> bio-oils must be up-graded to meet the requirements of the current infrastructure; carboxylic acids, hydroxyketones, hydroxy-aldehydes, phenolic compounds and dehydrosugars constitute the main oxygenated compounds in bio-oils. Accordingly, to achieve the desired composition an active catalyst must be applied here. Previous researches have already made great efforts in searching for an appropriate catalyst for up-grading bio-oils. Noble metal catalysts, such as Pd,<sup>4,5</sup> Ru,<sup>6,7</sup> Rh<sup>6</sup> and Pt<sup>8,9</sup> heterogeneous and homogeneous catalysts deposited on various supports have been employed for up-grading bio-oils, however, the limitations of high cost, coke deposition and low selectivity toward carbon–oxygen bonds made them an unsatisfactory choice. As alternatives to the noble metal catalysts, sulfide NiMo and CoMo catalysts<sup>10,11</sup> with various surface chemistries have also been widely researched, however, their application in industry is restricted by their low resistance to

deactivation and low energy efficiency caused by the severe reaction conditions. Other catalysts include: zeolites,<sup>12,13</sup> transition metal catalysts<sup>14</sup> and so on. Among these catalysts,  $\text{Mo}_2\text{C}$ -based catalysts have been extensively studied due to their inexpensive cost and platinum-like characteristics.<sup>15–17</sup> Additionally, their attractive properties such as coke resistance, high selectivity, water-stability and chemical stability<sup>18,19</sup> also make them excellent candidates for many reactions, such as hydrogenation,<sup>15</sup> hydrodesulfurization,<sup>20</sup> hydrocarbon isomerization,<sup>21</sup> methane reforming<sup>22</sup> and so on.

Our previous research concerning the high catalytic activity of  $\text{Mo}_2\text{C}$  supported on AC ( $\text{Mo}_2\text{C}/\text{AC}$ ) in the HDO of vegetable oils demonstrated that the permeated carbon in the lattice of the Mo metal caused elongation of the Mo–Mo distance and an increase in the d-band electron density at the Fermi level of molybdenum, which was proved to be effective for hydrogenation.<sup>23,24</sup>

In this paper, we used a carbothermal hydrogen reduction (CHR) method based on TPR to prepare  $\text{Mo}_2\text{C}/\text{AC}$  catalyst at 700 °C, and we explored the effects of different reaction conditions on the HDO of vanillin, which is one typical aldehyde compound produced during oil pyrolysis derived from the lignin fraction. The results of catalytic tests conducted at mild conditions in aqueous solution stated that the  $\text{Mo}_2\text{C}$ -based catalyst showed high selectivity toward C=O bonds, and possessed the properties of water-stability and coke resistance.

## 2. Experimental section

### 2.1 Materials

All reagents were commercially available and were used as supplied without further purification.  $\text{HNO}_3$ ,

Department of Chemistry, Xixi Campus, Zhejiang University, Hangzhou 310028, Zhejiang, P. R. China. E-mail: c224@zju.edu.cn; Fax: +86-571-88273283; Tel: +86-571-88273283

$(\text{NH}_4)_6\text{Mo}_7\text{O}_{24}\cdot 4\text{H}_2\text{O}$  (AHM), vanillin, raw activated carbon, ethanol, anisole, glucose and deionized water were used throughout the experiments.

## 2.2 Methods

### 2.2.1 Preparation of catalysts

**Catalyst preparation.** Supported on AC, the different loading of  $\text{Mo}_2\text{C}$  catalysts were accomplished using the CHR method. Prior to impregnation, the carbon was treated with  $\text{HNO}_3$  to remove amorphous carbon and to increase the number of surface oxygen-containing functional groups which was useful for the metal deposition and dispersion.<sup>25</sup> The pretreatment of the raw activated carbon was carried out by mixing raw activated carbon (4.00 g) and 6 M  $\text{HNO}_3$  (100.0 mL) at 80 °C for 3 hours. After the mixture being cooled to room temperature, the sample was washed with plenty of water and dried at 120 °C for one night. Incorporation of Mo onto the carbon support to prepare the catalysts with different loading of  $\text{Mo}_2\text{C}$  was completed by mixing activated carbon (2.00 g), the corresponding amount of AHM and 15 mL of deionized water in a 100 mL round-bottomed flask, followed by sonication at 120 W for 1.5 hours and removal of the water at 60 °C with a rotatory evaporator. The sample was then dried at 120 °C for 12 hours. All of these catalysts were carbonized at 700 °C to obtain the desired molybdenum phase. The carbonization process was performed in a  $\text{H}_2$  flow by heating to 450 °C from room temperature at the ramping rate of 5 °C  $\text{min}^{-1}$  and 1 °C  $\text{min}^{-1}$  from 450 °C to 700 °C, and holding for 2 hours at the final temperature. Before exposure to air, the catalyst was passivated in a flow of 1.0%  $\text{O}_2/\text{N}_2$  for 12 hours at room temperature. Herein, the as-synthesized catalyst was denoted as  $\text{Mo}_2\text{C}/\text{AC}$ , and the theoretical percentages of  $\text{Mo}_2\text{C}$  to carbon in the prepared catalysts were 10.0, 20.0, 30.0, 50.0 and 80.0%, respectively. The CHN analysis result revealed that the content of C, H and N in 20.0%  $\text{Mo}_2\text{C}/\text{AC}$  was 68.8, 0.75 and 0.64%, respectively. The theoretical content of C in 20.0%  $\text{Mo}_2\text{C}/\text{AC}$  was 84.0%, so the percentage carbon loss during the preparation was 47.1%. According to the previous reports,<sup>26</sup> in the process of preparing  $\text{Mo}_2\text{C}$  through a temperature-programmed reaction,  $\text{CH}_4$ , CO and  $\text{H}_2\text{O}$  would be released as gaseous products, which would account for the carbon loss. According to the CHN analysis, the actual content of  $\text{Mo}_2\text{C}$  in 20.0%  $\text{Mo}_2\text{C}/\text{AC}$  was 31.7%, but in this article we still denoted the catalyst as 20.0%  $\text{Mo}_2\text{C}/\text{AC}$ .

**Preparation of the bulk  $\text{Mo}_2\text{C}$  catalyst.** Glucose was employed as the carbon source in the preparation of the bulk  $\text{Mo}_2\text{C}$  catalyst. The CHR method was used with some modification to guarantee that the glucose was pyrolyzed to carbon. Specifically, the sample was heated to 400 °C at the rate of 5 °C  $\text{min}^{-1}$ , then 1 °C  $\text{min}^{-1}$  to 700 °C and held for 2 hours.

### 2.2.2 Experimental procedure

**HDO reactions.** All reactions were carried out in a 100 mL stainless steel autoclave equipped with a mechanical stirrer. For a typical run, the catalyst (0.050 g for the loaded catalyst, and 0.100 g for the bulk catalyst) was introduced into the reactor together with reagent (0.100 mmol of vanillin) and water (20.0 mL). Subsequently, the samples were heated to a temperature

range of 80–180 °C after being pressurized with hydrogen to a relevant pressure (0.6 MPa, 1.0 MPa, 2.0 MPa), and then reacted for a certain time.

**Regeneration of the catalyst.** The catalyst filtered from the mixture after reaction was refluxed in ethanol at 85 °C for 4 hours; the separated catalyst was treated at 290 °C in the flow of air for 2 hours to remove the adsorbate; then reduction of the catalyst was carried out at 700 °C for 2 hours in the flow of  $\text{H}_2$  using the CHR method, and the reduced catalyst was passivated in a flow of 1.0%  $\text{O}_2/\text{N}_2$  for 12 hours at room temperature.

**2.2.3 Analytical methods.** After each reaction, the gas products were collected and qualitatively analyzed on a GC (sp-6800A) equipped with a packed column (TDX-01), while the qualitative analysis of the liquid products was performed using GC-MS (HP 6890GC and 5973MSD) with a HP-5 column. Thereafter, with anisole as the internal standard, the quantitative analysis was carried out using high performance liquid chromatography (HPLC) equipped with Hypersil BDS ( $\text{C}_{18}$  chromatographic column with the diameter of 5  $\mu\text{m}$ , 150 mm  $\times$  4.6 mm) at an ultraviolet ray wavelength of 270 nm. The mass balance was defined as the molar ratio of products after the reaction to the total vanillin in the feed (mass balance =  $(P + M)/M_0$ , where  $P$  was the molar mass of the products,  $M$  was the amount of vanillin after the reaction and  $M_0$  was the amount of vanillin in the feed, respectively).

**2.2.4 Catalyst characterization.** Raman spectra were obtained using a LabRam HR800 at an excitation wavelength of 514.5 nm. X-ray diffraction (XRD) patterns were recorded on a RIGAKU/MAX2550/PC diffractometer using  $\text{Cu K}\alpha$  radiation ( $\lambda = 0.15406$  nm) at a scan rate of 5°  $\text{min}^{-1}$  over the range of 10° to 80°. Transmission electron microscopy (TEM) was performed with a FEI Tecnai F30 microscope at an accelerating voltage of 300 kV. The acidity of the catalysts was evaluated using  $\text{NH}_3$ -temperature-programmed desorption ( $\text{NH}_3$ -TPD) with a BEL CAT-B instrument. Before adsorption, the samples were activated in helium at 500 °C (10 °C  $\text{min}^{-1}$  ramp) for 1 hour, then cooled to 100 °C, and saturated with  $\text{NH}_3$  for 30 min. Subsequently, the samples were purged with He at 50 mL  $\text{min}^{-1}$  for 15 min to remove  $\text{NH}_3$  in the gas phase and in the physically adsorbed state, and then the temperature was increased to 550 °C at increments of 10 °C  $\text{min}^{-1}$ .

## 3. Results and discussion

### 3.1 Characterization of $\text{Mo}_2\text{C}/\text{AC}$ catalysts

The XRD patterns of the catalysts with different loading are shown in Fig. 1. In agreement with the standard XRD patterns of hexagonal close-packed  $\beta$ - $\text{Mo}_2\text{C}$ , the diffraction peaks located at 34.4°, 38.0°, 39.4°, 61.5° and 69.6°, illustrating that  $\beta$ - $\text{Mo}_2\text{C}$  was successfully formed at 700 °C. Additionally, using Scherrer's formula, the average size of the 20.0%  $\text{Mo}_2\text{C}/\text{AC}$  crystallites at (101) was 2.6 nm, which was in good agreement with the average value predicted by TEM (2.6 nm), while the value was 15.0 nm for 50.0%  $\text{Mo}_2\text{C}/\text{AC}$ , suggesting that the particle size increased with loading.

The TEM images of 20.0%  $\text{Mo}_2\text{C}/\text{AC}$  shown in Fig. 2, together with XRD results, revealed that the  $\text{Mo}_2\text{C}$  particles with an

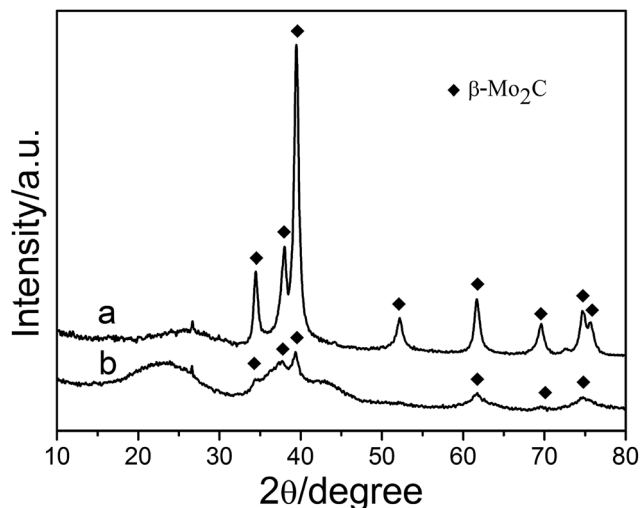


Fig. 1 XRD patterns of (a) 50.0% Mo<sub>2</sub>C/AC and (b) 20.0% Mo<sub>2</sub>C/AC.

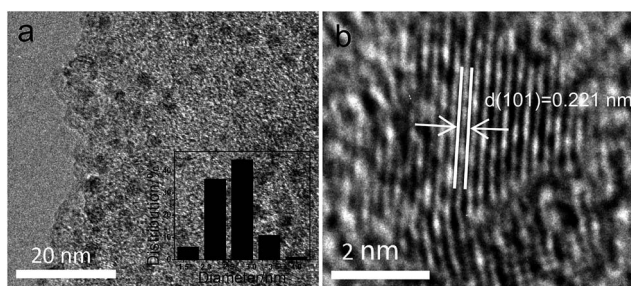


Fig. 2 TEM images and the diameter distribution of the 20.0% Mo<sub>2</sub>C/AC catalyst.

average diameter of 2.6 nm were well dispersed on the support. Fig. 2b showed the TEM micrographs of Mo<sub>2</sub>C with the *d*-spacing values of 0.221 nm for the (101) crystallographic planes.

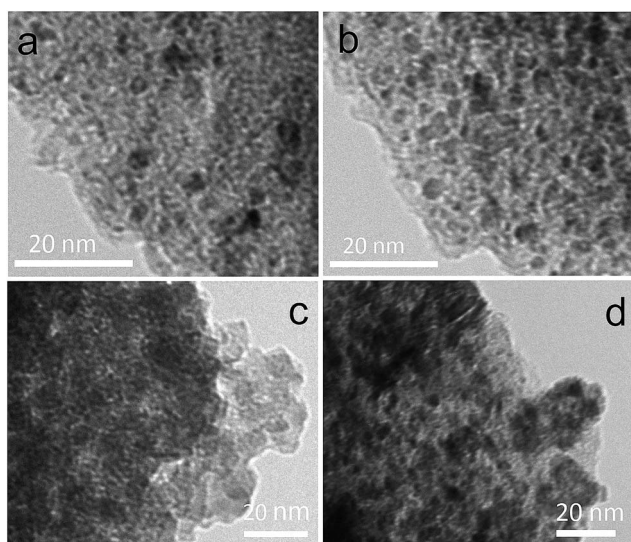


Fig. 3 TEM images (a–d) of the Mo<sub>2</sub>C/AC catalysts with a loading of 10.0, 30.0, 50.0 and 80.0%, respectively.

The TEM images of catalysts with different loading were shown in Fig. 3, from which it was easily concluded that the particles were well-distributed on the surface with low loading, while with increased loading the stacking of the particles resulted in agglomeration.

In the Raman spectra of 20.0% Mo<sub>2</sub>C/AC and untreated AC shown in Fig. 4, after loading, the increase in the intensity of the D band at  $\sim 1350$  cm<sup>-1</sup>, a defect-induced Raman feature revealing the imperfect crystalline structure of the material, was related to the oxygen-containing functional groups introduced by the treatment with HNO<sub>3</sub> and the passivation with 1.0% O<sub>2</sub>/N<sub>2</sub>.

Compared with AC, the NH<sub>3</sub>-TPD results displayed in Fig. 5 revealed that the 20.0% Mo<sub>2</sub>C/AC catalyst had a NH<sub>3</sub> desorption peak located at a temperature around 179 °C, indicating that the loading of active components imported weak acid sites, which could be explained by the presence of Mo–OH on the catalyst surface. Furthermore, according to previous reports, the weak acidity of the catalyst not only contributes to the adsorption of reactant and the process of hydrogenation, but also accounts for less mass balance.<sup>27</sup>

As can be seen in Table 1, the Brunauer–Emmett–Teller (BET) results of AC and the Mo<sub>2</sub>C/AC catalysts with different loading showed that loading of Mo<sub>2</sub>C caused the reduction of *S*<sub>BET</sub>, which was induced by the slight destruction of the AC surface in the carbonization procedure of preparing Mo<sub>2</sub>C. After loading, the pore volume increased within a certain range of loading due to the insertion of Mo<sub>2</sub>C particles, while with high loading the overlapping particles would block the pores and result in a decreased pore volume.

The N<sub>2</sub> adsorption–desorption isotherm of the Mo<sub>2</sub>C/AC catalyst is shown in Fig. 6. The isotherm was of type II according to IUPAC classification. The adsorption and desorption branches of the isotherm coincide, that is, there was no adsorption–desorption hysteresis. Depending on the surface properties of the catalyst, it can be considered as the stage of monolayer formation.

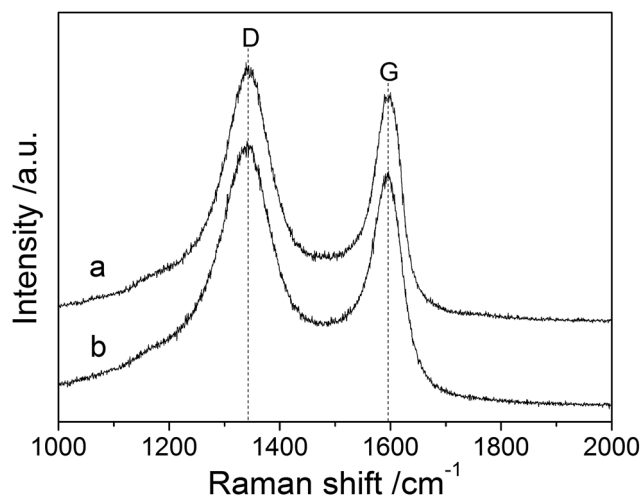


Fig. 4 Raman spectra of (a) 20.0% Mo<sub>2</sub>C/AC and (b) untreated AC.

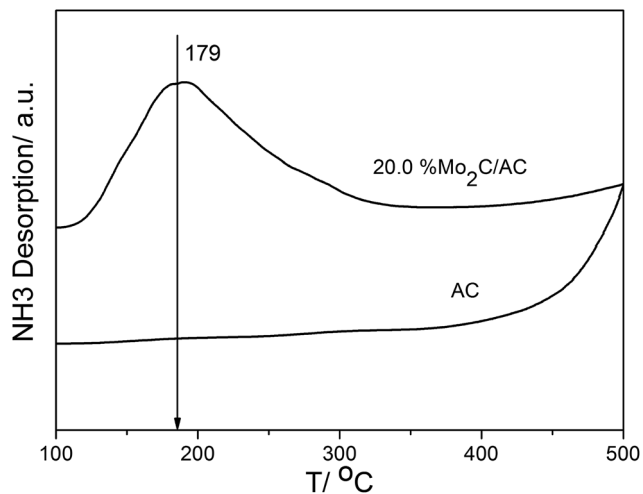


Fig. 5 NH<sub>3</sub>-TPD profiles of the 20.0% Mo<sub>2</sub>C/AC catalyst and AC.

Table 1 Textural parameters for AC and the Mo<sub>2</sub>C/AC catalysts with different loading

Sample	S <sub>BET</sub> (m <sup>2</sup> g <sup>-1</sup> )	Pore volume (cm <sup>3</sup> g <sup>-1</sup> )
AC	967	0.16
10.0% Mo <sub>2</sub> C/AC	945	0.26
20.0% Mo <sub>2</sub> C/AC	794	0.22
30.0% Mo <sub>2</sub> C/AC	683	0.14
50.0% Mo <sub>2</sub> C/AC	494	0.10
80.0% Mo <sub>2</sub> C/AC	418	0.07

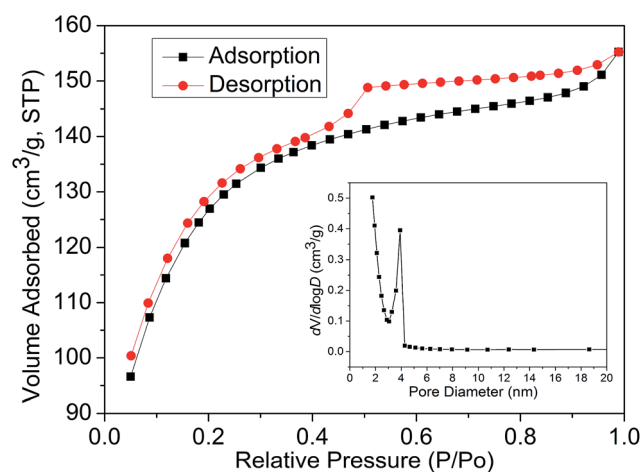


Fig. 6 Nitrogen adsorption-desorption isotherm of the 20.0% Mo<sub>2</sub>C/AC catalyst.

## 3.2 HDO of vanillin

**3.2.1 The blank reaction.** The blank experiment with no catalyst or AC was ran at 100 °C with 1.0 MPa of H<sub>2</sub> for 3 hours to verify the active part for this reaction. The results shown in Table 2 clearly indicated that the HDO reaction could not proceed without the catalyst and the effect of the AC was negligible.

**3.2.2 The distribution of products with time.** As can be seen in Fig. 7, in the first 1.5 hours, the reaction was accompanied by a rapid increase in the conversion of vanillin and yield of vanillyl alcohol, while a slow increase in the yield of *p*-creosol, suggesting that vanillin was mainly hydrogenated to vanillyl alcohol in the first step. As the reaction proceeded further, the main initial product, vanillyl alcohol, was gradually converted to *p*-creosol *via* hydrogenolysis; meanwhile, the conversion increased with time until it reached approximately 100%. Based on the experimental results, we speculated that the reaction was a consecutive reaction consisting of two first-order reactions. In the first step the vanillin adsorbed by acid sites was hydrogenated to vanillyl alcohol. The second step was completed by the hydrogenation and dehydration of vanillyl alcohol to *p*-creosol. Correspondingly, the HDO mechanism was proposed and shown in Fig. 8a, in which *p*-creosol was produced by a side reaction. Additionally, based on the small amount of CO detected in the gas products, the mechanism of the reaction to guaiacol was shown in Fig. 8b.

**3.2.3 The effect of different reaction conditions.** The experimental results of reactions catalyzed by the Mo<sub>2</sub>C/AC catalysts with different loading were shown in Fig. 9. With a 93.2% conversion of vanillin and a 50.1% yield of *p*-creosol under mild conditions (1.0 MPa, 100 °C, 3 h), the highest efficiency vanillin HDO reaction was achieved over the 20.0% Mo<sub>2</sub>C/AC catalyst. Associated with the increase in conversion of vanillin and yield of *p*-creosol, the increase in loading induced an increase in catalytic activity within a certain range of loading percentage, but no more increase was observed when the loading was higher than 50.0%. Based on the XRD and TEM results, it can be said that the stacking of the active particles accounted for the agglomeration and low catalytic activity. Compared with the result for catalysis by bulk Mo<sub>2</sub>C, the high activity of Mo<sub>2</sub>C/AC implied that the AC played a part in dispersing the active sites and changing the characteristics of the catalysts.

Results displayed in Fig. 10 demonstrated that the reaction temperature had a significant influence on the conversion of vanillin and yield of products. When the temperature rose from 80 °C to 100 °C, the conversion of vanillin improved remarkably from 51.4% to 98.6%, demonstrating that, at this range of temperature, the reaction was thermodynamically controlled. When conducted at temperatures higher than 100 °C, the increase in conversion with temperature was negligible, suggesting that the HDO reaction was under kinetic control at these conditions. The reaction temperature also had influence on the distribution of products. Hydrogenation of vanillin to vanillyl alcohol was the main reaction at a low temperature (80 °C), while, owing to the promoted rate of dehydration by the elevated reaction temperature, *p*-creosol with a yield of 63.7% became the dominating product at 100 °C. Further increasing of temperature offered an increase in the yield of *p*-creosol, as well as in the yield of guaiacol. A high yield of *p*-creosol of 82.0% was achieved at 180 °C. According to the previous reports, as the temperature elevated, the accelerated speed of dehydrogenation would cause an increase in polycondensation,<sup>28</sup> which was

Table 2 The results of the blank reaction<sup>a</sup>

Catalyst	Mass (g)	T (°C)	t (h)	Conv. (%)	Yield (%)		Mass balance (%)
					<i>p</i> -Creosol	Vanillin alcohol	
No	—	100	3	0	0	0	100
AC	0.05	100	3	3.0	0	3.0	100
Mo <sub>2</sub> C	0.10	150	6	33.8	12.9	17.1	99.9

<sup>a</sup> Reaction conditions: vanillin (0.1 mmol), water (20 mL),  $p(\text{H}_2) = 1.0$  MPa.

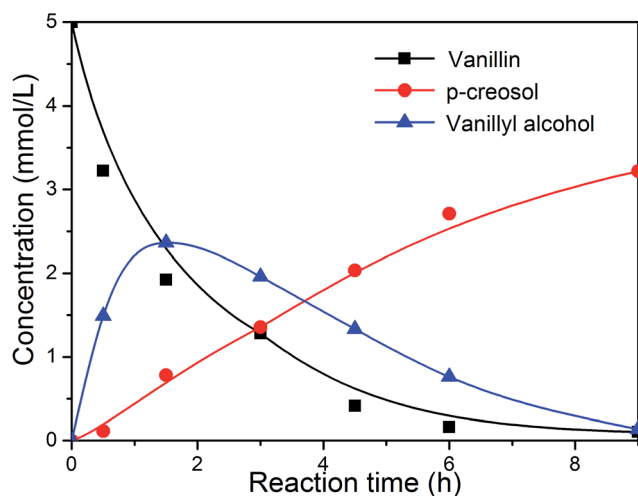


Fig. 7 The changes in the concentration of products and reactant over time in the presence of 50.0% Mo<sub>2</sub>C/AC at 100 °C and 0.6 MPa of H<sub>2</sub>.

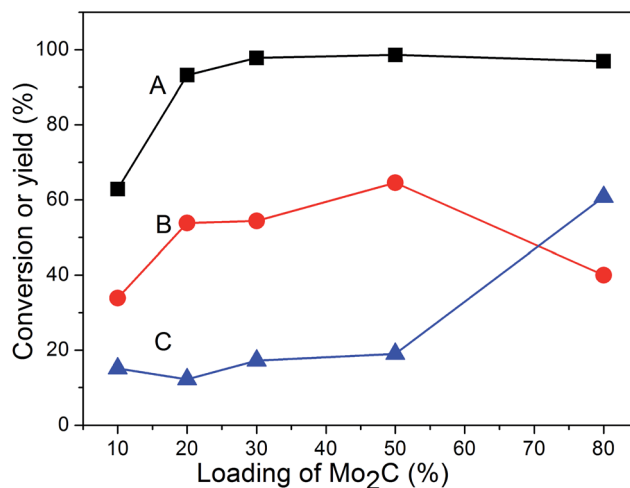


Fig. 9 The results for the reactions catalyzed by catalysts with different loading. Reaction conditions: 50.0% Mo<sub>2</sub>C/AC,  $p(\text{H}_2) = 1.0$  MPa, 100 °C for 3 hours. A is for the conversion of vanillin. B and C are for the yield of *p*-cresol and vanillyl alcohol, respectively.

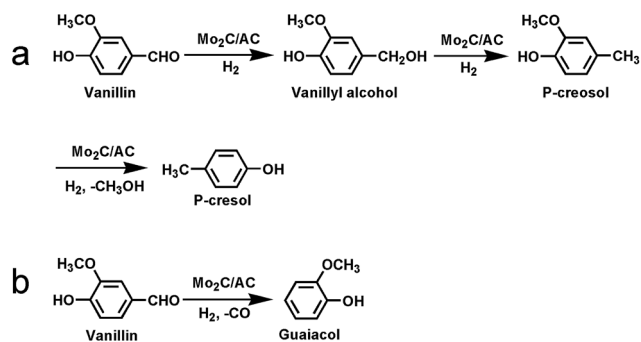


Fig. 8 The mechanisms of the vanillin HDO (a) and decarbonylation (b).

believed to be responsible for the loss in mass balance. Considering energy efficiency and distribution of products, the optimal temperature was at 100 °C.

To inspect the relationship between hydrogen pressure and the rate of hydrogenation, tests with the initial pressure from 0.6 MPa to 2.0 MPa were conducted at 100 °C for 3 hours. As shown in Fig. 11, the results indicated that increasing of hydrogen pressure could accelerate the step of dehydration to *p*-cresol significantly. However, the gradual increase in the conversion of vanillin and yield of *p*-cresol with the pressure increase from

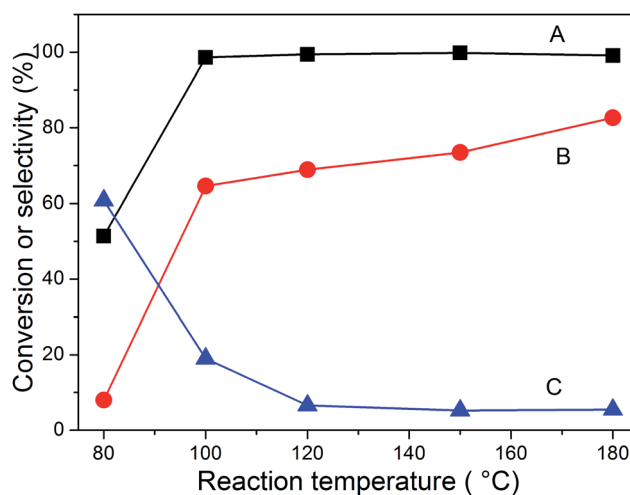


Fig. 10 Results of the reactions carried out at different reaction temperatures. Reaction conditions: 50.0% Mo<sub>2</sub>C/AC,  $p(\text{H}_2) = 1.0$  MPa, for 3 hours. A is for the conversion of vanillin. B and C are for the selectivity of *p*-cresol and vanillyl alcohol, respectively.

1.0 MPa to 2.0 MPa was attributed to the capacity for adsorption of hydrogen. In view of the equipment and the capacity for adsorption, the optimal hydrogen pressure was at 1.0 MPa.

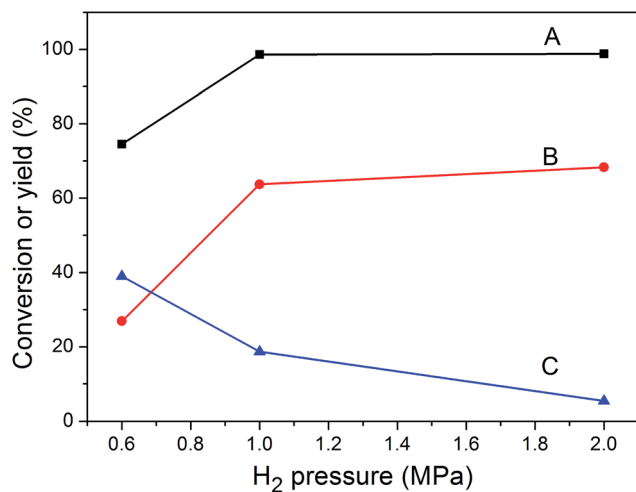


Fig. 11 The effect of H<sub>2</sub> pressure on the HDO reaction. Reaction conditions: 50.0% Mo<sub>2</sub>C/AC, 100 °C for 3 hours. A is for the conversion of vanillin. B and C are for the selectivity of *p*-creosol and vanillyl alcohol, respectively.

Table 3 The recycling results of the 20.0% Mo<sub>2</sub>C/AC catalyst<sup>a</sup>

Recycle times	Conv. (%)	Yield (%)				Mass balance (%)
		<i>p</i> -Creosol	Vanillyl alcohol	Guaiacol	<i>p</i> -Creosol	
1	99.6	57.4	2.40	0.30	3.60	67.1
2	99.5	53.7	3.20	0.9	6.90	65.1
3	99.3	52.9	6.90	1.70	6.90	68.9
4	99.1	49.9	11.8	2.40	5.30	70.4
5	99.4	52.3	6.63	1.01	6.90	67.4

<sup>a</sup> Reaction conditions: vanillin (0.2 mmol), catalyst (0.10 g), water (40 mL), *p*(H<sub>2</sub>) = 2.0 MPa, 100 °C, 3 h.

**3.2.4 The reutilization of catalyst.** The recycling of the 20.0% Mo<sub>2</sub>C/AC catalyst was carried out at 100 °C, 2.0 MPa of H<sub>2</sub> for 3 hours. The results are shown in Table 3. After being reused several times, the activity loss of the Mo<sub>2</sub>C/AC catalyst was negligible, indicating that the catalyst was stable, coke resistant and had promising prospects in industrial application.<sup>29,30</sup>

In this reaction, it was difficult to achieve 100% mass balance due to the instability of vanillin. Our research indicated that the loss in mass balance was mainly caused by the following reasons. Firstly, vanillin was easily polymerized to an oligomer which was difficult to quantify. Some of the oligomers were deposited on the catalyst, whereas others were in the separate phase. When a high concentration of vanillin participated in this reaction at the same conditions, a transparent, colorless polymer was obtained. The adsorption of products by the catalyst also contributed to the loss in mass balance.

## 4. Conclusions

The Mo<sub>2</sub>C catalysts with good crystalline structure were directly synthesized by a CHR method at a relatively low temperature

and were highly dispersed on the support. Taking the experimental results and energy efficiency into account, the optimal conditions for the HDO reaction catalyzed by the Mo<sub>2</sub>C/AC catalyst were considered to be a temperature of 100 °C, 1.0 MPa of H<sub>2</sub> for 3 hours, and 20.0% for catalyst loading. The Mo<sub>2</sub>C/AC catalysts were shown to have the character of water-stability, and high selectivity to the C=O bond under mild conditions. Moreover, due to the fact that it can be recycled several times with slight loss of activity, it can be said that the Mo<sub>2</sub>C/AC catalyst is coke resistant and possesses promising prospects for being used for up-grading bio-oil in the future.

## Acknowledgements

This work was financially supported by the National Basic Research Program of China (2013CB228104).

## Notes and references

- 1 M. Balat, *Energy Convers. Manage.*, 2011, **52**, 858–875.
- 2 A. Demirbas, *Energy Convers. Manage.*, 2008, **49**, 2106–2116.
- 3 A. D. Bulusheva and J. R. H. Rossa, *Catal. Today*, 2011, **171**, 1–13.
- 4 W. Yu, Y. Tang, L. Mo, P. Chen, H. Lou and X. Zheng, *Catal. Commun.*, 2011, **13**, 35–39.
- 5 Y. Tang, W. Yu, L. Mo, H. Lou and X. Zheng, *Energy Fuels*, 2008, **22**, 3484–3488.
- 6 L. Chen, Y. Zhu, H. Zheng, C. Zhang and Y. Li, *Appl. Catal., A*, 2012, **411**, 95–104.
- 7 J. Wildschut, I. Melian-Cabrera and H. J. Heeres, *Appl. Catal., B*, 2010, **99**, 298–306.
- 8 K. Murata, Y. Liu, M. Inaba and I. Takahar, *Energy Fuels*, 2010, **24**, 2404–2409.
- 9 H. Olcay, A. V. Subrahmanyam, R. Xing, J. Lajoie, J. A. Dumesic and G. W. Huber, *Energy Environ. Sci.*, 2013, **6**, 205–216.
- 10 Y. Liu, R. Sotelo-Boyás, K. Murata, T. Minowa and K. Sakanishi, *Energy Fuels*, 2011, **25**, 4675–4685.
- 11 A. Popov, E. Kondratieva, L. Mariey, J. M. Goupil, J. El Fallah, J. P. Gilson and F. Maugé, *J. Catal.*, 2013, **297**, 176–186.
- 12 A. G. Gayubo, A. T. Aguayo, A. Atutxa, R. Aguado, M. Olazar and J. Bilbao, *Ind. Eng. Chem. Res.*, 2004, **43**, 2619–2626.
- 13 J. Peng, P. Chen, H. Lou and X. Zheng, *Bioresour. Technol.*, 2009, **100**, 3415–3418.
- 14 C. Zhao, J. He, A. A. Lemonidou, X. Li and J. A. Lercher, *J. Catal.*, 2011, **280**, 8–16.
- 15 S. T. Oyama, *Catal. Today*, 1992, **15**, 179–200.
- 16 A. P. E. York, J. B. Claridge, A. J. Brungs, S. C. Tsang and M. L. H. Green, *Chem. Commun.*, 1997, 39–40.
- 17 J. R. Kitchin, J. K. Nørskov, M. A. Barteau and J. G. Chen, *Catal. Today*, 2005, **105**, 66–73.
- 18 P. Delporte, F. Meunier, C. Pham-Huu, P. Vennegues, M. J. Ledoux and J. Guille, *Catal. Today*, 1995, **23**, 251–267.
- 19 M. J. Ledoux, C. P. Huu, J. Guille and H. Dunlop, *J. Catal.*, 1992, **134**, 383–398.
- 20 K. R. McCrea, J. W. Logan, T. L. Tarbuck, J. L. Heiser and M. E. Bussell, *J. Catal.*, 1997, **171**, 255–267.

- 21 V. Keller, P. Wehrer, F. Garin, R. Ducros and G. Maire, *J. Catal.*, 1995, **153**, 9–16.
- 22 D. C. LaMont and W. J. Thomson, *Chem. Eng. Sci.*, 2005, **60**, 3553–3559.
- 23 Y. Qin, P. Chen, J. Duan, J. Han, H. Lou, X. Zheng and H. Hong, *RSC Adv.*, 2013, **3**, 17485–17491.
- 24 J. Han, J. Duan, P. Chen, H. Lou, X. Zheng and H. Hong, *ChemSusChem*, 2012, **5**, 727–733.
- 25 V. Z. Radkevich, T. L. Senko, K. Wilson, L. M. Grishenko, A. N. Zaderko and V. Y. Diyuk, *Appl. Catal., A*, 2008, **335**, 241–251.
- 26 C. Liang, P. Ying and C. Li, *Chem. Mater.*, 2002, **14**(7), 3148–3151.
- 27 P. M. Mortensen, J. D. Grunwaldt, P. A. Jensen, K. G. Knudsen and A. D. Jensen, *Appl. Catal., A*, 2011, **407**, 1–19.
- 28 E. Furimsky and F. E. Massoth, *Catal. Today*, 1999, **52**, 381–495.
- 29 J. Han, J. Duan, P. Chen, H. Lou and X. Zheng, *Adv. Synth. Catal.*, 2011, **353**, 2577–2583.
- 30 J. Han, J. Duan, P. Chen, H. Lou, X. Zheng and H. Hong, *Green Chem.*, 2011, **13**, 2561–2568.